An Experimental Investigation of Reactive Absorption of Carbon Dioxide into an Aqueous NH₃/H₂O/NaOH Solution

Ahad Ghaemi[1*], Vahid Hashemzadeh[2], and Shahrokh Shahhosseini[3]

[1] Assistant Professor, Process Simulation and Control Research Laboratory, Department of Chemical Engineering, Iran University of Science and Technology, Tehran, Iran
[2] M.S. Student, Process Simulation and Control Research Laboratory, Department of Chemical Engineering, Iran University of Science and Technology, Tehran, Iran
[3] Professor, Process Simulation and Control Research Laboratory, Department of Chemical Engineering, Iran University of Science and Technology, Tehran, Iran

Abstract

In this research, the reactive absorption of carbon dioxide in an aqueous solution of NH_3, H_2O, and NaOH has experimentally been investigated. The experiments were carried out in an absorption pilot plant in different operational conditions. The composition and temperature of both gas and liquid phases were obtained during the column height. The concentration of molecular and ionic species in the liquid phase was calculated using the principles of electrolyte and Pitzer model. In the experiments, the effect of sodium hydroxide concentration on carbon dioxide absorption was considered. The results revealed that the concentrations of ionic and molecular species in the liquid phase drastically influence the absorption rate of carbon dioxide. Also, the results showed that the absorption rate of carbon dioxide was increased by increasing ammonia and sodium hydroxide concentration.

Keywords: Reactive Absorption, Electrolytes, Sodium Hydroxide, Ammonia, Carbon Dioxide

1. Introduction

Among the greenhouse gases, carbon dioxide (CO_2) is the most influential gas on global warning. There are various techniques used for the removal of CO_2, including reactive absorption, membrane separation, biological fixation, and hydrate base separation (Gaspar et al., 2011; Norouzbahari et al., 2016; Pashaei et al., 2017). Reactive absorption seems to be the most practical and effective technique. Reactive absorption is an important unit of several chemical and petrochemical industries. Chemical reactions in the absorption of undesirable gases bring many advantages in terms of operating conditions such as increasing mass transfer while decreasing the operating total pressure (Schneider et al., 2003; Khan et al., 2011; Pashaei et al., 2016).

Recently several important industrial reactive absorption processes have been successfully investigated both theoretically and experimentally by a number of researchers. A wide variety of chemical solvents

* Corresponding Author:
    Email: aghaemi@iust.ac.ir

have been employed, where aqueous solutions of alkanolamines have found comparatively widespread applications (Pacheco and Rochelle, 1998). Recently, mixed solutions including blend amines and hydroxide solutions are used in the absorption of undesired gases (Ghaemi et al., 2011).

Usually reactive absorption processes occur in the aqueous electrolyte solutions (Ahmadi et al, 2008). In these solutions, the components are in ionic and molecular form, whereas in the gas phase the components are only in molecular form (Ghaemi et al., 2009). The ionic species affect the amount of acidity and basicity of the liquid phase, which has an impact on the absorption rate of the gases, especially on acidic and basic gases like CO_2 and NH_3. In the previous researches, the effects of all species in the liquid phase on the absorption of gas components have not been considered (Ghaemi et al., 2011b; Noeres et al., 2003).

An experimental investigation of reactive absorptions can lead to better understanding of the process behavior and designing more efficient operating conditions (Ghaemi et al., 2011c). Therefore, in this work, a procedure is introduced to study the reactive absorption of CO_2 in an aqueous electrolyte solution of NH_3, H_2O, and $NaOH$ applying the principles of electrolyte solutions (Beutier and Renon, 1978). In addition, all ionic and molecular species concentration profiles along the column height have been obtained. Furthermore, the influence of ionic and molecular species on the absorption rate of CO_2 has experimentally been studied.

2. Modeling of electrolyte systems

According to works of Edwards et al., thermodynamic modeling of electrolyte solutions is based on three principles (Edwards et al., 1978; Etemad et al., 2015):

1- Overall mass balance of electrolytes in liquid phase:

$$m_A = m_a + \frac{(m_+ + m_-)}{2} \tag{1}$$

2- Electroneutrality:

Electrolyte solutions are electrically neutral even though they may contain millions of charged ions (cations and anions). This means that the molar concentration of positive charges in an electrolyte solution always equals the molar concentration of negative charges. Equation 2 mathematically represents this principle:

$$\sum_{i=1}^{c} \left|(z^+)_i\right| (m_{M^{z+}})_i = \sum_{j=1}^{c'} \left|(z^-)_j\right| (m_{X^{z-}})_j \tag{2}$$

3- Chemical equilibria:

Equilibria of chemical reactions taking place in the solution (dissociation of water and electrolytes and reactions between electrolytes and/or products of their dissociation) with the deviations from the ideal solution properties taken into account (Kontogeorgis and Folas, 2009):

$$K_r = \prod_{i=1}^{} m_i^{v_{ir}} \gamma_i^{v_{ir}} \qquad \begin{cases} i = 1, 2, \dots \\ r = 1, 2, \dots \end{cases} \tag{3}$$

where, K is the association equilibrium constant of reaction r, and v_{ir} is the stoichiometric coefficient of i in reaction r; m_i and γ_i respectively represent the molality and activity coefficients of i.

Deviations of aqueous electrolyte solution properties from the ideal solution properties are expressed by the means of the excess Gibbs free energy G^E. The classical way of calculating the activity coefficients of real species dissolved in the solution is based on the semi-empirical Pitzer equation for G^E (Pitzer and Mayorga, 1973; Pitzer, 1973):

$$G^E \Big/ (n_w RT) = f_1(I) + \sum_i \sum_j \left\{ \beta_{ij}^{(0)} + \beta_{ij}^{(1)} f_2(I) \right\} m_i m_j + \sum_i \sum_j \sum_k \mu_{ijk} m_i m_j m_k \tag{4}$$

where, $f_1(I)$ is the Debye–Huckel–Pitzer function describing the effect of long-range ion–ion electrostatic interactions depending on the ionic strength of the solution. $\beta_{ij}^{(0)}$ and $\beta_{ij}^{(1)}$ are the parameters of binary short-range intermolecular interactions. $f_2(I)$ is a function describing the effect of ionic strength, on binary short-range intermolecular interactions. μ_{ijk} is the parameter of ternary short-range intermolecular interactions. Differentiation of Equation 4 yields the activity coefficient of the dissolved species i (Kamps et al., 2000; Norouzbahari et al., 2015):
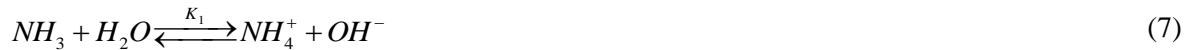
$$\begin{aligned}
\ln \gamma_i^{(m)} = &-A_\phi z_i^2 \left[\frac{\sqrt{I}}{1+b\sqrt{I}} + \frac{2}{b} \ln(1+b\sqrt{I}) \right] + \\
&2 \sum_{j \neq W} m_j \left[\beta_{ij}^{(\circ)} + \beta_{ij}^{(1)} f_2(x_1) + \beta_{ij}^{(2)} f_2(x_2) \right] - \\
&z_i^2 \sum_{j \neq W} \sum_{k \neq W} m_j m_k \left[\beta_{jk}^{(1)} f_3(x_1) + \beta_{jk}^{(2)} f_3(x_2) \right] + 3 \sum_{j \neq W} \sum_{k \neq W} m_j m_k \tau_{ijk}
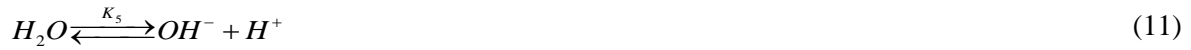\end{aligned} \tag{5}$$

The activity of water follows the Gibbs–Duhem equation:

$$\ln a_W = M_W \left[\begin{array}{l} 2A_\phi \dfrac{I^{1.5}}{1+b\sqrt{I}} - 2\sum_{i \neq W} \sum_{j \neq W} \sum_{k \neq W} m_i m_j m_k \tau_{ijk} - \\ \sum_{i \neq W} \sum_{j \neq W} m_i m_j \left(\beta_{ij}^{(\circ)} + \beta_{ij}^{(1)} e^{-x_1} + \beta_{ij}^{(2)} e^{-x_2} \right) - \sum_{i \neq W} m_i \end{array} \right] \tag{6}$$

3. Reactive absorption of CO_2 in an $NaOH/NH_3/H_2O$ system

When CO_2 is absorbed in an $NaOH/NH_3/H_2O$ solution, the following chemical reaction equilibria in the liquid phase occur: the protonation of ammonia (R1), the formation of bicarbonate (R2), the dissociation of bicarbonate to carbonate (R3), the formation of carbamate from ammonia and bicarbonate (R4), the autoprotolysis of water (R5), and the dissolution of NaOH (Brettschneider et al., 2004; Ghaemi et al., 2011).

$$NH_3 + H_2O \underset{\longleftarrow}{\overset{K_1}{\longrightarrow}} NH_4^+ + OH^- \tag{7}$$

$$CO_2 + H_2O \underset{\longleftarrow}{\overset{K_2}{\longrightarrow}} HCO_3^- + H^+ \tag{8}$$

$$HCO_3^- \underset{\longleftarrow}{\overset{K_3}{\longrightarrow}} H^+ + CO_3^{2-} \tag{9}$$

$$NH_3 + HCO_3^- \underset{\longleftarrow}{\overset{K_4}{\longrightarrow}} NH_2COO^- + H_2O \tag{10}$$

$$H_2O \xrightleftharpoons{K_5} OH^- + H^+ \tag{11}$$

$$NaOH \rightarrow Na^+ + OH^- \tag{12}$$

The model of the present system consists of the flowing equations:

1- Mass balances of the electrolytes:

$$\bar{m}_{NH_3} = m_{NH_3} + m_{NH_4^+} + m_{NH_2COO^-} \tag{13}$$

$$\bar{m}_{CO_2} = m_{CO_2} + m_{CO_3^{-2}} + m_{HCO_3^-} + m_{NH_2COO^-} \tag{14}$$

$$\bar{m}_W = m_W + m_{OH^-} + m_{CO_3^{-2}} + m_{HCO_3^-} \tag{15}$$

2- Charge balance in the solution:

$$m_{NH_4^+} + m_{H^+} + m_{Na^+} = m_{OH^-} + 2m_{CO_3^{-2}} + m_{HCO_3^-} + m_{NH_2COO^-} \tag{16}$$

3- Equilibria of chemical reactions:

$$K_1 = \frac{\left(m_{NH_4^+}\gamma_{NH_4^+}\right)\left(m_{OH^-}\gamma_{OH^-}\right)}{\left(m_{NH_3}\gamma_{NH_3}\right)a_W} \tag{17}$$

$$K_2 = \frac{\left(m_{HCO_3^-}\gamma_{HCO_3^-}\right)\left(m_{H^+}\gamma_{H^+}\right)}{\left(m_{CO_2}\gamma_{CO_2}\right)a_W} \tag{18}$$

$$K_3 = \frac{\left(m_{CO_3^{-2}}\gamma_{CO_3^{-2}}\right)\left(m_{H^+}\gamma_{H^+}\right)}{\left(m_{HCO_3^-}\gamma_{HCO_3^-}\right)} \tag{19}$$

$$K_4 = \frac{\left(m_{NH_2COO^-}\gamma_{NH_2COO^-}\right)a_W}{\left(m_{NH_3}\gamma_{NH_3}\right)\left(m_{HCO_3^-}\gamma_{HCO_3^-}\right)} \tag{20}$$

$$K_5 = \frac{\left(m_{OH^-}\gamma_{OH^-}\right)\left(m_{H^+}\gamma_{H^+}\right)}{a_W} \tag{21}$$

In the liquid phase, there are ten molecular and ionic species, including NH_3, CO_2, H_2O, Na^+, NH_4^+, HCO_3^-, CO_3^{2-}, H^+, OH^-, and NH_2COO^-. The activity coefficients of these species were obtained using Equations 5 and 6. The temperature dependence of dissociation equilibrium constants are determined using the correlations reported elsewhere (Ghaemi et al., 2011c).

4. Absorption pilot plant

The schematic of the applied absorption pilot plant is shown in Figure 1. The column is made of a glass cylinder with a diameter of 105 mm containing three packing sections. A tray is mounted between these sections to redistribute the liquid flow. On each tray, two temperature sensors are installed to measure gas and liquid temperatures. Liquid and gas samples can also be taken using two valves, which are

installed on the trays. The packing beads are ceramic Rasching rings with a diameter of 0.5 inches. Gas and liquid samples are taken at four points of the column as shown in Figure 1. Temperatures are measured at four positions along the column to give temperature profiles for gas and liquid phases.
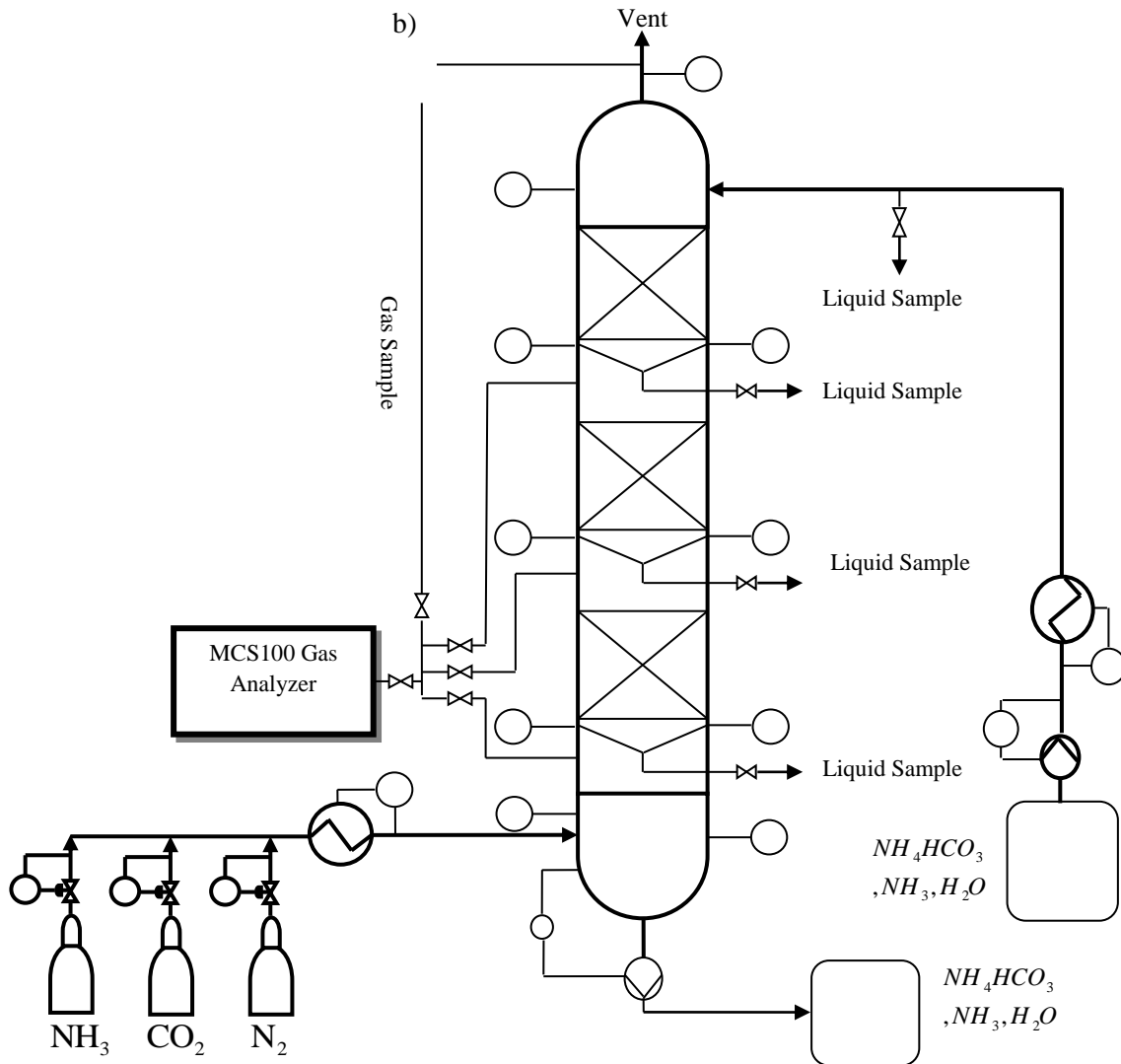

Figure 1
a) An image of the absorption pilot plant used in this work, and b) a schematic of the pilot plant.

5. Experiments

The experimental data were obtained in steady state conditions at atmospheric pressure. At the beginning of the experiments, only nitrogen gas was fed to the column, and then liquid and the other gases feed flow rates and temperatures were adjusted to the desired values by four flowmeters. After reaching a steady-state condition, which was indicated by a steady-state temperature profile and fixed concentration of the analyzer, the gas and liquid samples were taken. Duplicate liquid and gas samples were taken with a time interval of about 10 minutes. Gas samples were sent to an online gas analyzer and liquid samples were analyzed offline.

The pilot plant experiments have been carried out in different conditions in terms of inlet liquid phase concentrations. Liquid flow rate was 80 lit/hr. for all of the experiments. The inlet and outlet conditions of the absorption column are given in Table 1.

For testing the repeatability of the conducted experimental runs, one experimental run was repeated for three times, and a standard deviation equal to 0.0015 was obtained for CO_2 mole fraction at top of the column (gas outlet), which indicates satisfactory repeatability.

Table 1
Operating conditions of the absorption column in two different experiments.

Process Parameter	Experiment 1		Experiment 2	
	Feed	**Outlet**	**Feed**	**Outlet**
Gas				
Temperature (C)	13.1	14.0	13.5	14.0
NH$_3$ (mol/hr.)	0.00	0.41	0.00	0.407
CO$_2$ (mol/hr.)	14.87	12.12	14.84	12.46
N$_2$ (mol/hr.)	208.25	208.25	207.82	207.82
H$_2$O (mol/hr.)	0.0	7.65	0.0	7.88
Liquid				
Temperature (C)	12.8	13.5	13.1	13.4
NH$_3$ (mol/m^3)	149.28	145.87	149.40	146.06
CO$_2$ (mol/m^3)	27.0	61.5	28.5	54.9
NaOH (mol/m^3)	16.7	16.7	16.7	16.7

6. Measurements

The liquid samples were analyzed offline with an ion chromatography (IC-762 type from Metrohm Company) based on the conductivity detection method. As mentioned above, the results are averages of the two samples taken in the same condition but at different times. Here, the average deviation for the determination of CO_2 and NH_3 was given in the range of 4–6%. The online gas analyzer is a MCS100 from SICKMAIHAK Company, which is an extremely compact multi-component infrared photometer for extractive continuous monitoring of flue gases. In this process, H_2O, NH_3, and CO_2 concentrations were measured in the gas phase. The response time of MCS100 analyzer is less than 2 seconds with average measurement deviation of less than 2% for NH_3 and CO_2.

7. Results and discussion

The experiments were carried out in a steady state condition. Table 2 shows temperatures and component concentrations of both liquid and gas phases. The solubility of carbon dioxide in aqueous solutions is very different. The experiments were conducted to study the impacts of liquid feed concentration and liquid and gas temperature on CO_2 absorption. The results of Table 2 reveal that the absorption of CO_2 increases as a result of a decrease in the liquid feed temperature. The experiments showed that increasing NaOH concentration in the inlet liquid, increases CO_2 absorption during the column height. It is clear that at a high concentration of NaOH in the liquid phase, the concentration of hydroxide ion is high, so reaction rate between CO_2 and hydroxide will increase. Therefore, as Table 2 shows the absorption rate is increased by increasing NaOH concentration.

Table 2
Temperatures and component concentrations of pilot plant experiment.

Experiment 1

Z	Partial pressure(kPa)				Temp.	Temp.	Mole/Liter		
(m)	PN_2	PCO_2	PNH_3	PH_2O	$TG(°C)$	$TL(°C)$	NH_3	CO_2	NaOH
1.0	0.9091	0.0545	0.0018	0.0345	14.0	13.1	0.1494	0.0285	0.0167
0.5	0.9027	0.0620	0.0013	0.0339	13.6	14.0	0.1485	0.0487	0.0167
0.2	0.8963	0.0664	0.0009	0.0364	14.0	14.2	0.1478	0.0610	0.0167
0.0	0.9333	0.0667	0.0000	0.0000	13.5	13.4	0.1461	0.0549	0.0167

Experiment 2

Z	Partial pressure(kPa)				Temp.	Temp.	Mole/Liter		
(m)	PN_2	PCO_2	PNH_3	PH_2O	$TG(°C)$	$TL°C)$	NH_3	CO_2	NaOH
1.0	0.9262	0.0380	0.0009	0.0348	13.7	13.0	0.0040	0.0000	0.2674
0.5	0.9101	0.0536	0.0015	0.0348	12.8	13.6	0.0052	0.0309	0.2674
0.2	0.9002	0.0637	0.0012	0.0348	12.7	13.9	0.0047	0.0516	0.2674
0.0	0.9333	0.0667	0.0000	0.0000	12.7	13.5	0.0023	0.0528	0.2674

Experiment 3

Z	Partial pressure(kPa)				Temp.	Temp.	Mole/Liter		
(m)	PN_2	PCO_2	PNH_3	PH_2O	$TG(°C)$	$TL(°C)$	NH_3	CO_2	NaOH
1.0	0.9273	0.0326	0.0015	0.0385	14.1	13.2	0.0065	0.0000	0.3003
0.5	0.9061	0.0533	0.0015	0.0390	13.7	14.1	0.0065	0.0411	0.3003
0.2	0.8989	0.0605	0.0014	0.0391	13.6	14.2	0.0064	0.0558	0.3003
0.0	0.9333	0.0667	0.0000	0.0000	13.5	14.0	0.0036	0.0629	0.3003

Experiment 4

Z	Partial pressure(kPa)				Temp.	Temp.	Mole/Liter		
(m)	PN_2	PCO_2	PNH_3	PH_2O	$TG(°C)$	$TL(°C)$	NH_3	CO_2	NaOH
1.0	0.9317	0.0268	0.0018	0.0402	14.2	13.3	0.0089	0.0000	0.3197
0.5	0.9006	0.0579	0.0016	0.0399	14.1	14.6	0.0087	0.0615	0.3197
0.2	0.8935	0.0654	0.0015	0.0396	13.7	14.7	0.0085	0.0769	0.3197
0.0	0.9333	0.0667	0.0000	0.0000	13.6	14.4	0.0056	0.0739	0.3197

Experiment 5

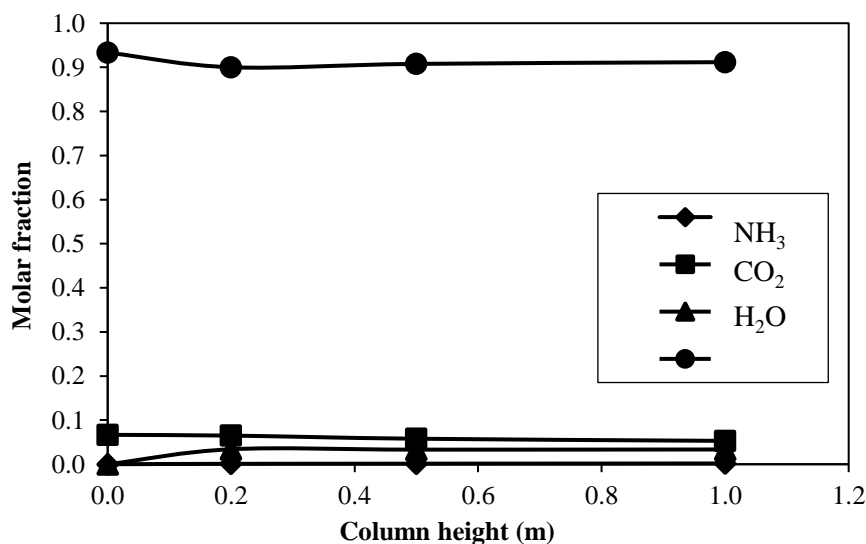| Z	Partial pressure(kPa)				Temp.	Temp.	Mole/Liter		
(m)	PN_2	PCO_2	PNH_3	PH_2O	$TG(°C)$	$TL(°C)$	NH_3	CO_2	NaOH
1.0	0.9365	0.0208	0.0018	0.0409	14.3	13.4	0.0111	0.0000	0.3362
0.5	0.9066	0.0514	0.0016	0.0404	13.6	14.5	0.0109	0.0596	0.3362
0.2	0.8942	0.0633	0.0015	0.0410	13.9	14.8	0.0107	0.0840	0.3362
0.0	0.9333	0.0667	0.0000	0.0000	13.7	14.6	0.0078	0.0851	0.3362

Figure 2
Gas phase mole fractions along the column height.

Figure 2 shows component mole fractions in gas phase along the column height for Experiment 1. CO_2 is gradually transferred to the liquid phase throughout the column, while water and ammonia are transferred from liquid to gas phase. As a result, nitrogen partial pressure in the gas phase is decreased. Water vapor concentration curve in Figure 2 shows that there is no water in the gas feed although when the gas phase enters the column, its water content starts to rise due to the mass transfer from the liquid phase to the gas phase. Since the sum of all mole fractions equals 1, nitrogen concentration is descending

at the bottom of the column and ascending at other sections as a result of the variations in the concentrations of the other components in the gas phase.
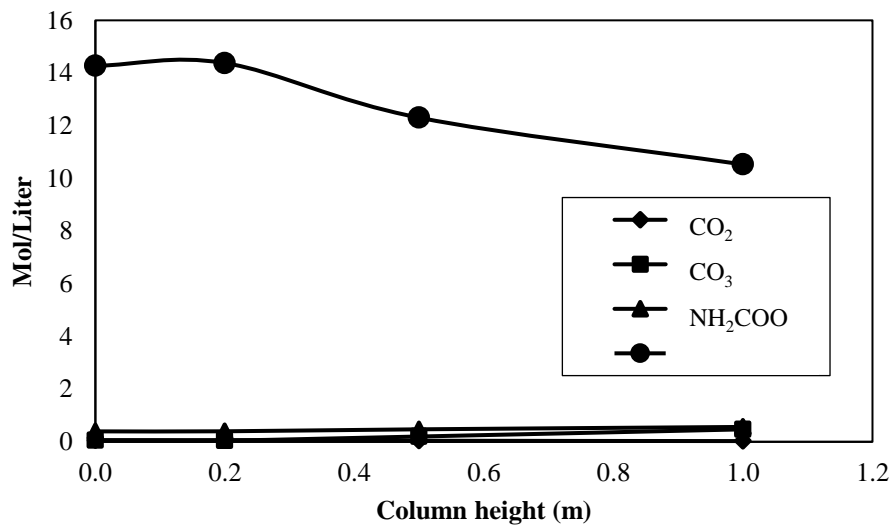

Figure 3
Ionic and molecular concentration of carbon dioxide species along the column in Experiment 1.

In the liquid phase, there are molecular and ionic species, and the compositions are obtained using the equations of electrolyte systems. Figures 3 and 4 show molecular and ionic carbon dioxide species concentrations. According to these figures, when liquid move from top to bottom of the column, molecular CO_2 and HCO_3^- concentrations increase duo to an increase in CO_2 absorption from gas phase. On the other hand, CO_3^{-2} and NH_2COO concentrations decrease due to chemical reactions. From $z=0.2$ to $z=0$, CO_3^{-2} and NH_2COO concentrations increase because of the decomposition of CO_2 and HCO_3^- species. In the electrolyte systems, the concentration of CO_2, because of chemical reactions, is low, so in this system, as show in Figure 4, the concentration of CO_2 is low.
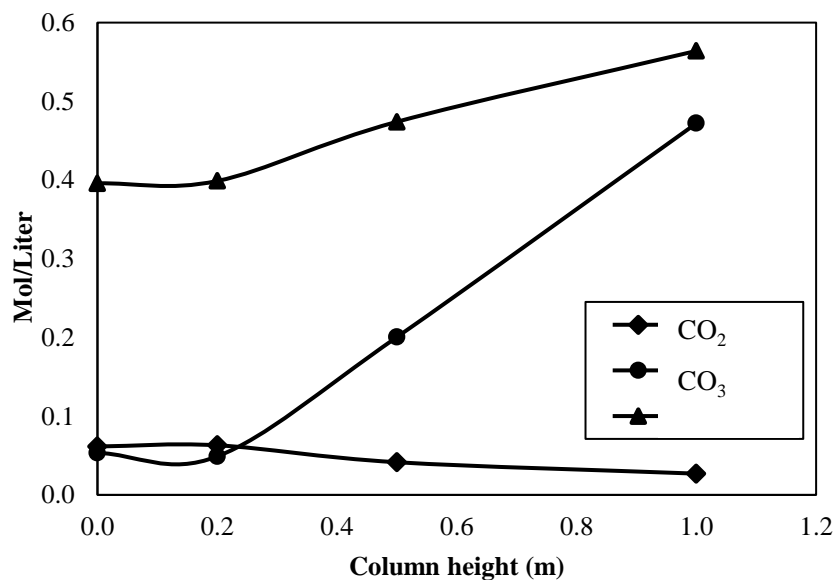

Figure 4
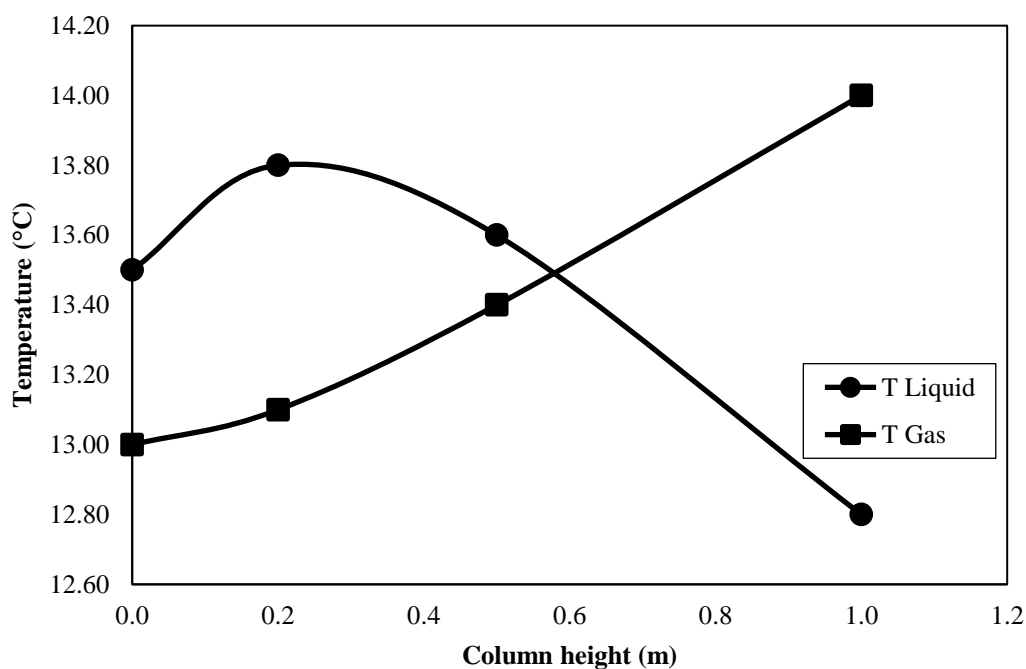Ionic and molecular concentration of carbon dioxide species along the column in Experiment 1.

Figure 5
Temperature gradients of liquid and gas phases along the column height in Experiment 2.

The absorption of CO_2 is exothermic, causing high variation in temperature of both phases in the first section of the column (0-0.2 m). In this section, reaction heat increases liquid phase temperature, and because liquid and gas phases are in close contact, the gas phase temperature is also increased. The temperature gradients for both phases are shown in Figure 6. Between the column height of 0.2 and 0.4 m, the temperature of liquid phase has a maximum, and in this point the absorption rate is high.
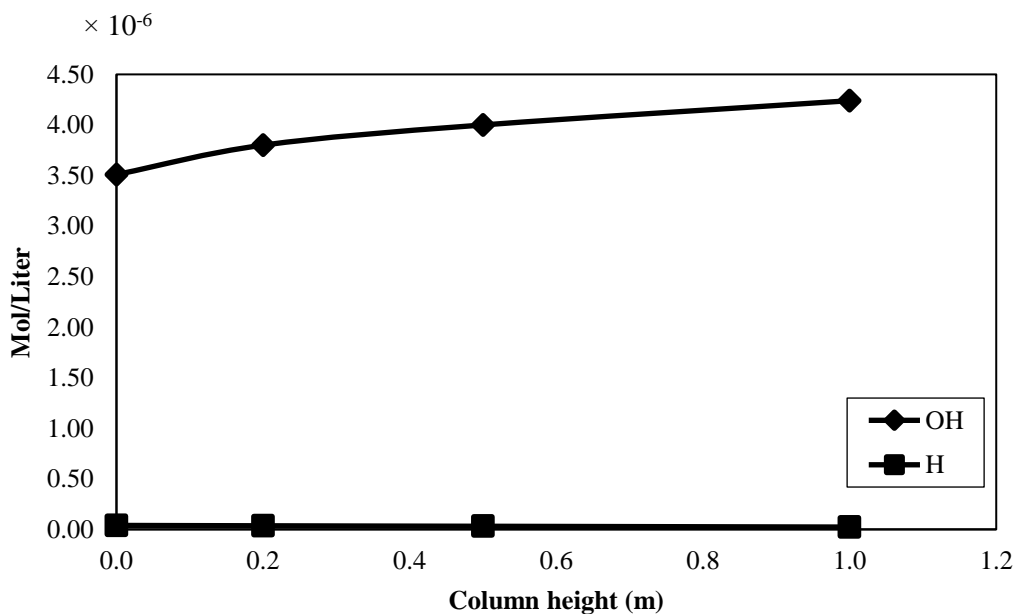

Figure 6
The acidity and basicity of solution along the column height in Experiment 2.

Figure 6 indicates the acidity and basicity of the liquid phase along the column height. Mixed ammonia and sodium hydroxide solution is a basic solution, and the concentration of OH$^-$ is higher than that of H$^+$. Therefore, the inlet solution is basic, and, due to the absorption of acidic gas (CO_2), the basicity of the solution decreases, which in turn leads to a lower rate of CO_2 absorption.

8. Conclusions

In this work, the reactive absorption of carbon dioxide in an aqueous solution of NH_3, H_2O, and NaOH was experimentally investigated. The electrolyte principles of aqueous solutions were used to calculate the concentrations of the ionic and molecular components in the liquid phase. The experiments were conducted to obtain the data employing a pilot plant packed bed absorption column. The results revealed that carbon dioxide absorption occurred gradually throughout the column. The data also indicated that carbon dioxide absorption rate strongly depended on the concentrations of free ammonia and hydroxide ion. Finally, the results showed that CO_2 absorption rate was increased by increasing sodium hydroxide concentration.

Nomenclature

a_W	:Activity of water
G	:Gibbs energy
I	:Ionic strength
K	:Association equilibrium constant
m	:Molarity
M	:Water molecular weight
n	:Mole number
R	:World gas constant
T	:Temperature
γ_i	:Activity coefficients of species i
Superscript	
E	:Excess characteristic
Subscripts	
A	:Ammonia group
a	:Molecular aqueous solutions
c	:Carbon dioxide group
-	:Anion
+	:Cation
i, j, and k	:Components
w	:Water

References

Ahmadi, M., Gomes, V. G., and Ngian, K., Advanced Modelling in Performance Optimization for Reactive Separation in Industrial CO_2 Removal, Separation and Purification Technology, Vol. 63, No. 107, 2008.

Brettschneider, O., Thiele, R., Faber, R., Thielert, H., and Wozny, G., Experimental Investigation and Simulation of the Chemical Absorption in a Packed Column for the System NH_3–CO_2–H_2S–$NaOH$–H_2O, Separation and Purification Technology, Vol. 39, p. 139, 2004.

Beutier, D. and Renon, H., Representation of NH_3-H_2S-H_2O, NH_3-CO_2-H_2O, and NH_3-SO_2 -H_2O Vapor-liquid Equilibria, Industrial Engineering Chemical Processing Design and Development, Vol. 17, p. 220, 1978.

Edwards, T. J., Maurer, G., Newman, J., and Prausnitz, J. M., Vapor-liquid Equilibria in Multicomponent Aqueous Solutions of Volatile Weak Electrolytes, AIChE Journal, Vol. 24, p. 966 1978.

Etemad, E., Ghaemi A., and Shirvani M., Rigorous Correlation for CO_2 Mass Transfer Flux in Reactive Absorption Processes, International Journal of Greenhouse Gas Control, Vol. 42, p. 288, 2015.

Gaspar, J. and Cormos A.M., Dynamic Modeling and Validation of Absorber and Desorber Columns for Post-combustion CO_2 Capture, Computer Chemical Engineering, Vol. 35, p. 2044, 2011.

Ghaemi, A., Shahhosseini, Sh, and Ghannadi M., Experimental Investigation of Reactive Absorption of Ammonia and Carbon Dioxide by Carbonated Ammonia Solution, Iranian Journal of Chemistry and Chemical Engineering Research, Vol. 30, p. 2, 2011.

Ghaemi, A., Sh., Shahhosseini, and Ghannadi M., Nonequilibrium Dynamic Modeling of Carbon Dioxide Absorption by Partially Carbonated Ammonia Solutions, Chemical Engineering Journal, Vol. 149, p. 110, 2009.

Ghaemi, A., Torab-Mostaedi M., and Ghannadi, M., Nonequilibrium Dynamic Modeling of Simultaneous Reactive Absorption of Gases, Journal of Taiwan Institute Chemical Engineering, Vol. 42, p. 173, 2011b.

Ghaemi, A., Ghannadi, M., and Mostaedi, M., Kinetics and Absorption Rate of CO_2 into Partially Carbonated Ammonia Solutions, Chemical Engineering Communication, Vol. 198, p. 1169, 2011c.

Noeres, C., Kenig, E. Y., and Gorak A., Modeling of Reactive Separation Processes: Reactive Absorption and Reactive Distillation, Chemical Engineering Processing, Vol. 42, p. 157, 2003.

Norouzbahari, S., S. Shahhosseini, and Ghaemi A., Chemical Absorption of CO_2 into an Aqueous Piperazine (PZ) Solution: Development and Validation of a Rigorous Dynamic Rate-based Model, RSC Advances, Vol. 6, p. 240017, 2016.

Norouzbahari, S., Shahhosseini S., and Ghaemi A., CO_2 Chemical Absorption into Aqueous Solutions of Piperazine: Modeling of Kinetics and Mass Transfer Rate, Journal of Natural Gas Science and Engineering, Vol. 26, p. 1059, 2015.

Kamps, A., Sing, R., Rumpf, B., and Maurer, G., Influence of NH_4C_l, NH_4NO_3, and $NaNO_3$ on the Simultaneous Solubility of Ammonia and Carbon Dioxide in Water, Journal of Chemical Engineering Data, Vol. 45, p. 796, 2000.

Khan, F. M., Krishnamoorthi V., and Mahmud T., Modeling Reactive Absorption of CO_2 in Packed Columns for Post-combustion Carbon Capture Applications, Chemical Engineering Research and Design, Vol. 89, p. 1600, 2011.

Kontogeorgis, G. M., and Folas, G. K., Thermodynamic Models for Industrial Applications: from Classical and Advanced Mixing Rules to Association Theories: Wiley, 2009.

Pacheco, M. A. and Rochelle G. T., Rate-based Modeling of Reactive Absorption of CO_2 and H_2S into Aqueous Methyldiethanolamine, Industrial Engineering Chemical Research, Vol. 37, p. 4107, 1998.

Pashaei, H., Ghaemi A., and Nasiri M., Experimental Investigation of CO_2 Removal Using Piperazine Solution in a Stirrer Bubble Column, International Journal of Greenhouse Gas Control, Vol. 63, p. 226, 2017.

Pashaei, H., Ghaemi A., and Zarandi M.N., Modeling and Experimental Study on the Solubility and Mass Transfer of CO_2 into Aqueous DEA Solution Using a Stirrer Bubble Column, RSC Advances, Vol. 6, p. 108075, 2016.

Pitzer, K. S., Thermodynamics of Electrolytes. I. Theoretical Basis and General Equations, Journal of Physics and Chemistry, Vol. 77, p. 268, 1973.

Pitzer, K. S. and Mayorga, G., Thermodynamics of Electrolytes II: Activity and Osmotic Coefficients for Strong Electrolytes with One or Both Ions Univalent, Journal of Physics and Chemistry, Vol. 77, p. 2300,1973.

Schneider, R., Sander, F., and Gorak A., Dynamic Simulation of Industrial Reactive Absorption Processes, Chemical Engineering Processing, Vol. 42, p. 955, 2003.